引用格式：YANG Fei, LI Mengmeng, GAO Lanlan. Single Longitudinal Mode 589 nm Laser in Composite-cavity[J]. Acta Photonica Sinica, 2021, 50(5):0514004
杨飞,李萌萌,高兰兰. 基于复合腔的单纵模589 nm激光器[J].光子学报,2021,50(5):0514004

基于复合腔的单纵模589 nm激光器

杨飞,李萌萌,高兰兰
(长春理工大学 理学院,长春 130022)

摘　要:介绍了一种LD泵浦Nd:YVO_4和Nd:YAG的单纵模589 nm激光器。1 064 nm与1 319 nm的基频光通过"L"型复合谐振腔获得同时振荡,通过Ⅱ类相位匹配切割的KTP晶体腔内和频以及由布鲁斯特片和KTP组成的双折射滤波器的选频,获得了单纵模589 nm连续激光器。利用琼斯矩阵方法分析了两个基频光的S偏振和P偏振光通过双折射滤波器时的损耗。结果表明:1 064 nm和1 319 nm次纵模的损耗分别比峰值透射率纵模的损耗大0.5%和2%以上。以此为基础,在实验上实现了一种单纵模589 nm激光器,其最大输出功率为58 mW,功率稳定性优于0.36%,线宽约为30 MHz。双折射滤波器方法对双波长振荡及和频激光器实现单纵模输出是一种有效的方法。

关键词:激光;和频;双折射滤波器;单纵模;连续波;复合腔
中图分类号:TN248.1　　**文献标识码**:A　　**doi**:10.3788/gzxb20215005.0514004

Single Longitudinal Mode 589 nm Laser in Composite-cavity

YANG Fei, LI Mengmeng, GAO Lanlan
(*College of Science*, *Changchun University of Science and Technology*, *Changchun* 130022, *China*)

Abstract: A laser-diode pumped Nd: YVO_4 and Nd: YAG single-longitudinal-mode 589 nm laser is presented. The fundamental waves of 1 064 nm and 1 319 nm simultaneously oscillate through an L type composite resonator. Through intracavity sum-frequency-generation in a KTP crystal (cut at type II phase matching), the single longitudinal mode 589 nm continuous wave is obtained by a birefringent filter which is consisted of a Brewster plate and the KTP crystal. The losses of S- and P- elements of the two fundamental waves are calculated by Jones matrix method. The losses of the first sub-longitudinal modes for 1 064 nm and 1 319 nm are 0.5% more and 2% more than their peak transmission modes respectively. Based on the above mentioned, a single-longitudinal-mode 589 nm laser is realized in experiment. The maximum output power is 58 mW, the amplitude fluctuation is less than 0.36%, and the line width is about 30 MHz. The results show that the birefringent filter technology is effective for single-longitudinal-mode double-wavelength oscillation and sum-frequency-generation lasers.

Key words: Laser; Sum-frequency-generation; Birefringent filter; Single-longitudinal-mode; Continuous wave; Composite resonator
OCIS Codes: 140.3570; 140.3580; 190.2620

Foundation item: Jilin Province Department of Education "13th five-year" Science and Technology Research Planning Project (No. JJKH20190552KJ)
First author: YANG Fei (1996—), male, M.S. degree candidate, mainly focuses on solid state laser. Email: yangfei57517@163.com
Supervisor(**Contact author**): GAO Lanlan (1974—), female, professor, Ph.D. degree, mainly focuses on nonlinear optics and solid state laser. Email: 865781943@qq.com
Received: Nov.17, 2020; **Accepted**: Jan.9, 2021

0 Introduction

Laser Diode (LD) pumped all-solid-state lasers have the advantages of high efficiency, long lifetime, compactness, and good liability[1-3]. The low-noise and Single-Longitudinal-Mode (SLM) 589 nm lasers are extensively required by biomedicine, sodium laser guiding star, city view and scientific research[4-8]. Due to the spatial hole-burning effect, the solid-state lasers generally operate in Multi-Longitudinal-Mode (MLM), and the coupling between the longitudinal modes during the nonlinear frequency conversion process will cause the irregular fluctuation in laser output power. In previous reports, there were several ways to realize the SLM[9], laser generation such as the twisted mode cavity[10], microchip cavity[11], inserting etalon[12], ring cavity[13-14], birefringent filtering technology[15], and so on. The SLM 589 nm lasers have been realized through the scheme of out-of-cavity Sum-Frequency Generation (SFG) and Raman doubling frequency[16-20]. The birefringence filter technology has been successfully used in frequency doubling lasers. However, few reports have been presented about this technology in SFG laser, which is mainly due to suppressing sub-longitudinal modes oscillating for two fundamental waves in a SFG laser is more difficult than that for one fundamental wave in a Second Harmonic Generation (SHG) laser.

To obtain a highly stable, compact and narrow linewidth 589 nm laser, a composite-cavity laser with intracavity SFG is designed in this paper. The longitudinal-mode-selective mechanism of birefringence filter for double-wave oscillation is analyzed in theory. An SLM 589 nm laser is accomplished by birefringence filter in experiment. A Nd:YVO_4 crystal is used to achieve 1 064 nm fundamental wave, and a Nd:YAG crystal is used to generate 1 319 nm fundamental wave. A linear cavity and an L type cavity are coupled by a flat-concave mirror. The birefringent filter composed of a Brewster Plate (BP) and a KTP crystal is placed in the overlap sub-cavity.

1 Theoretical analysis

The longitudinal-mode-selective theory of birefringent filter can be analyzed by solving the eigenvalue of the Jones matrix [21]. The configuration of the SLM laser achieved by birefringence filter technology is shown in Fig. 1. It is composed of a laser crystal, a BP and a KTP nonlinear crystal. The KTP crystal cut at type II critical phase matching is located near the output mirror M and acts as both SFG crystal and wave plate.

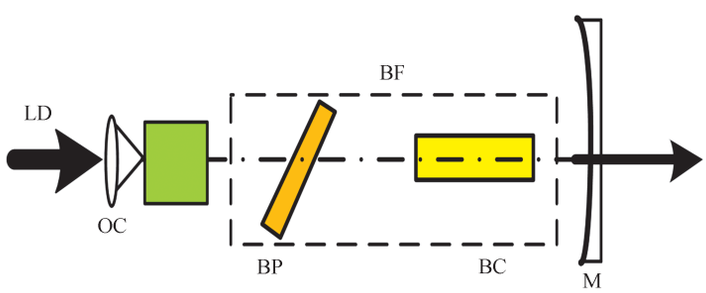

Fig.1 Schematic diagram of birefringence filter

By assuming that the Jones matrix of the laser crystal, KTP crystal and BP are $\boldsymbol{W}_1$, $\boldsymbol{W}_2$ and $\boldsymbol{P}$ respectively, the Jones matrix of the fundamental wave in the cavity for one round trip can be expressed as

$$\boldsymbol{M}=\boldsymbol{W}_1\times\boldsymbol{P}\times\boldsymbol{R}(-\theta)\times\boldsymbol{W}_2\times\boldsymbol{W}_2\times\boldsymbol{R}(\theta)\times\boldsymbol{P}\times\boldsymbol{W}_1 \tag{1}$$

where, $\boldsymbol{W}_1=\begin{pmatrix}1 & 0\\ 0 & \mathrm{e}^{\delta_1}\end{pmatrix}$, $\boldsymbol{W}_2=\begin{pmatrix}1 & 0\\ 0 & \mathrm{e}^{\delta_2}\end{pmatrix}$. δ_1, δ_2 are the relative phase delay of the laser crystal and the KTP crystal respectively; $\delta_i=\dfrac{2\pi}{\lambda}\Delta nd$, in which λ is the wavelength of the fundamental wave of 1 064 nm or 1 319 nm, Δn is the refractive index difference of the fundamental waves in the crystals (laser crystal and KTP correspond to 0.2, 0.08 respectively), and d is the crystal length. $\boldsymbol{P}=\begin{pmatrix}q & 0\\ 0 & 1\end{pmatrix}$, and $q=\left[2n/\left(1+n^2\right)\right]^2$, in which n is the

refractive index of BP at fundamental waves: $n_{1064}=1.473$, $n_{1319}=1.472$. $\boldsymbol{R}(\theta)=\begin{pmatrix}\cos\theta & \sin\theta\\ \sin\theta & \cos\theta\end{pmatrix}$ is the coordinate conversion matrix between the laser crystal and the KTP crystal (laser crystal is S-P coordinate system, KTP is o-e coordinate system), and θ is the angle between *s*-*p* and *o*-*e* coordinate systems. The fundamental waves are linear polarized after passing through the BP. When the polarized direction of the incident fundamental wave coincides with the P polarization plane of the BP, the losses suffering from the BP would be zero. These fundamental wavelengths are called peak transmission wavelength. The KTP crystal is placed at 45° on the horizontal plane. The optical axis of the KTP crystal is parallel to the crystal plane and the angle with the polarized direction of the fundamental waves is 45°, which is $\theta=45^{\circ}$. By solving the eigenequation of $\boldsymbol{MA}=\zeta\boldsymbol{A}$ (where $\boldsymbol{A}$ is the ray matrix of incident fundamental wave), the eigenvalues of $\boldsymbol{M}$, $\zeta_{1,2}$, can be obtained. The intensity transmission of the fundamental waves is given by the square of the modulus of the eigenvalue. The birefringence filter transmission at different fundamental wavelengths can be solved. The laser crystal is 3 mm long and the sum frequency crystal KTP is 7 mm long. The transmission curves of the S and P polarized fundamental waves are shown in Fig. 2 and Fig. 3 respectively. The Fig. 2 shows the transmission curves of 1 064 nm fundamental wave when the BP is placed at an angle of 55.827°. The Fig. 3 shows the transmission curves of 1 319 nm fundamental wave when the BP is placed at an angle of 55.310°. The upper convex curve is the transmission for the P polarized element, and the lower concave curve is the transmission for the S polarized element. It can be seen from the figures that the losses of the S polarized elements are larger (losses range from 57% ~ 67%) than those for P polarized elements (losses range from 0% ~ 15%). When the laser wavelengths are 1 063.63nm and 1 319.2 nm, the losses are zero for P polarized elements.

Based on the total length of the resonant cavities (the linear cavity is 75 mm long and the L type cavity is 80 mm long), the contiguous longitudinal wavelength intervals of 1064 nm and 1319 nm are about 0.006 9 nm and 0.011 nm respectively. For the P polarized elements the losses of the first sub-longitudinal modes of both fundamental waves (as shown in Fig. 2 and Fig. 3) are 0.5% and 2% respectively. Therefore, if the losses difference is large enough the peak transmission fundamental wave mode would oscillate and the others will be suppressed and the SLM laser can be realized. According to the Fresnel formula, the refractive indexes of the quartz crystal BP for the two fundamental waves are: $n_{1064}=1.473$, $n_{1319}=1.472$. The Brewster angle are: $\theta_{B1064}=55.827^{\circ}$, $\theta_{B1319}=55.310^{\circ}$, and the angle difference is 0.517°. The tiny difference between these two fundamental waves makes it reasonable to realize SLM for two fundamental waves at the same time.

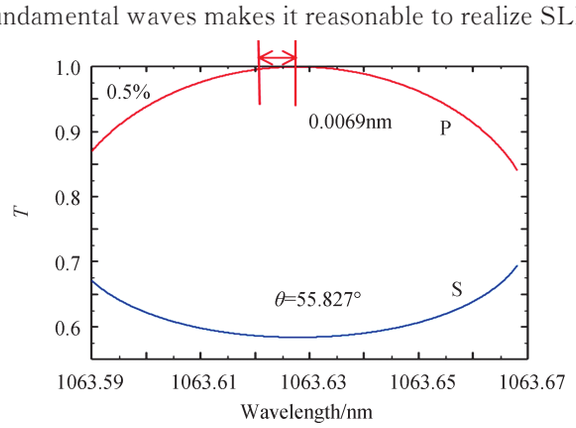

Fig.2 1064 nm wavelength transmission as a function of wavelength

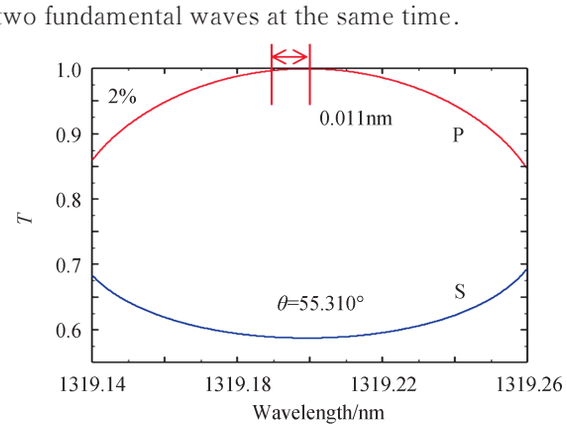

Fig.3 1319 nm wavelength transmission as a function of wavelength

2 Experimental study

Fig.4 shows the schematic diagram of experimental setup. The laser diode (LD1) has a maximum output power of 4.68 W, and center wavelength of 808 nm. The pump power is focused by using the coupling system (OC1) into the center of the Nd:YVO_4 crystal ($3\times3\times3$ mm^3, Nd^{3+} doping concentration 1at.%). The Nd:YVO_4 is wrapped in indium foil and mounted in a copper slot. The left flat side surface of the laser crystal is coated with High Transmission (HT) at 808 nm and high refection (HR) at 1 064 nm, acting as the input

mirror for 1 064 nm. The right flat side surface is coated with Anti-Reflection (AR) at 1 064 nm. The maximum output power of the laser diode (LD2) is 2.34 W and the center wavelength is also 808 nm. The pump power is focused by using another coupling system (OC2) into the center of the Nd:YAG crystal (3×3×3 mm^3, Nd^{3+} doping concentration 1at.%). The Nd:YAG crystal is wrapped in indium foil and mounted in a copper slot too. The incident flat side surface of laser crystal is coated with HT at 808 nm and HR at 1319 nm, acting as the input mirror for 1 319 nm. The output flat side is coated with AR at 1 319 nm. A flat-curvave mirror M3 with a curvature radius of 200 mm is placed in the cavity as a beam splitter. The concave surface is coated with HR (at 1 310～1 340 nm and 808 nm) and AR (at 650～670 nm and 1 064 nm). The planar surface is coated with AR at 650 nm～ 670 nm and 1064 nm. The output mirror M4 is a flat-concave mirror with a curvature radius of 100 mm. The concave surface is coated with HR at 1 319 nm/1 064 nm and HT at 589 nm. The flat surface is coated with HT at 589 nm. Both ends surface of the sum frequency crystal KTP (3×3×7 mm^3) are coated with HT at 1 319 nm, 1 064 nm and 589 nm. The thermoelectric coolers (TEC1 and TEC2) are used to control the temperature of the LDs and the resonant cavity to ensure the stable operation of the laser. The BP (uncoated), with a thickness of 2 mm, is placed at a Brewster angle.

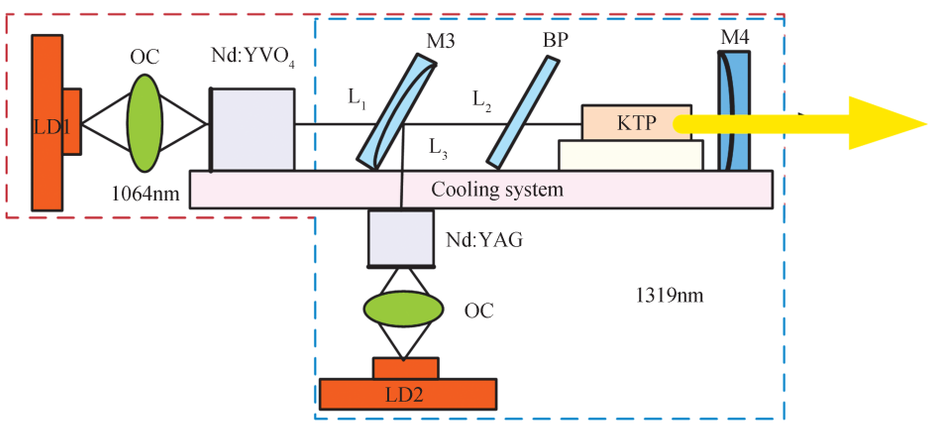

Fig.4 Laser experimental device diagram

First, the longitudinal mode conditions of 1 064 nm and 1 319 nm are measured with a Fabry-Perot (F-P) scanning interferometer (SA210-8B, 10G, Thorlabs). When there is no BP in the cavity, the 1 064 nm laser operates in multimode and 1 319 nm operates in less longitudinal mode, as shown in Fig. 5(a) and (c) respectively. The reason is that the pump power for 1 319 nm is lower than that for 1 064 nm. When the BP is placed in the cavity and fine-tuned with angle, SLM oscillations of both 1 064 nm and 1 319 nm lasers are realized, as shown in Fig.5 (b) and (d). The line width of the 1 064 nm and 1 319 nm are 262 MHz and 240 MHz respectively. The experimental results illustrate that one BP method is effective for 1 064 nm and 1 319 nm to realize the SLM oscillation.

Second, the longitudinal mode states at 589 nm are detected. The KTP crystal is placed near the output coupler. The position and angle of the KTP crystal are adjusted to obtain high conversion efficiency. It is found that the 589 nm laser is operating in multimode at all pumping energy level when the laser is oscillating without BP in the cavity. Fig.6 shows the F-P interferometer scanning spectrum of MLM 589 nm laser when the Nd:YVO_4 is pumped with 2.1 W and Nd:YVG is pumped with 1.3 W.

Third, the BP is put on the left side of the KTP crystal near the beam splitter. The position and angle of the BP is tuned until SLM exist at every Free Spectral Range (FSR) of the F-P analyzer and no any other sub-longitudinal modes appears. The results are shown in Fig. 7(a). With an F-P interferometer (SA200-5B, Thorlabs) the spectral line-width of the 589 nm laser is measured. The FSR of the interferometer is 1.5 GHz with a minimum fineness of 200 and a finer resolution of 7.5 MHz. The spectral line-width of SLM 589 nm laser at the maximal output level is 30 MHz (As shown in Fig.7(b)). The line spectrum of SLM 589 nm is shown in Fig.8.

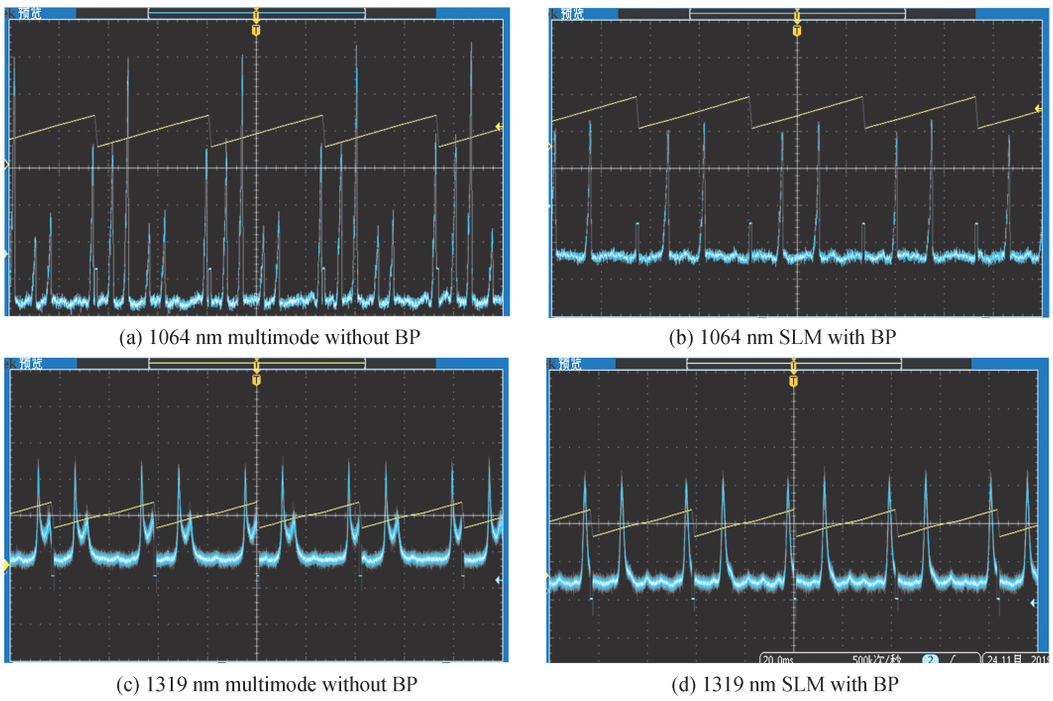

(a) 1064 nm multimode without BP (b) 1064 nm SLM with BP

(c) 1319 nm multimode without BP (d) 1319 nm SLM with BP

Fig.5 The longitudinal mode of 1064 nm and 1319 nm

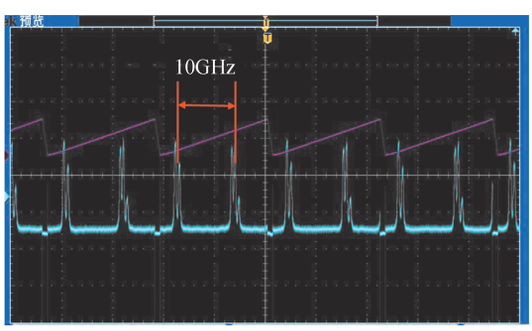

Fig.6 589 nm multimode with maximum pump power

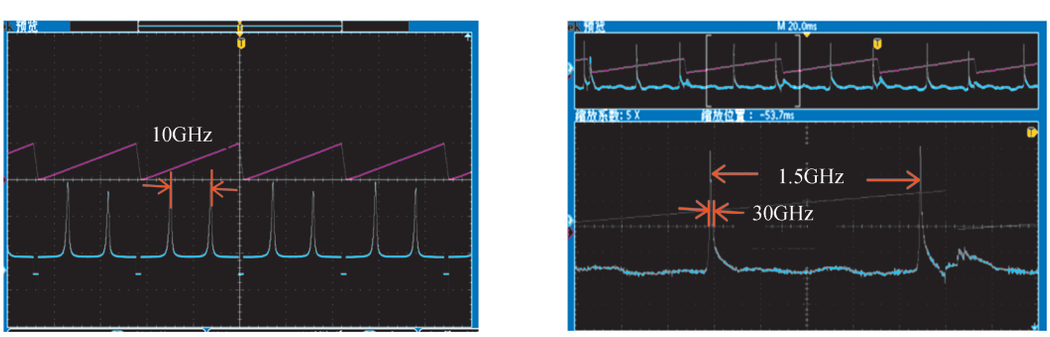

(a) 589 nm SLM measured by 10 GHz interferometer (b) 589 nm SLM measured by 1.5 GHz interferometer

Fig.7 Spectral analysis of 589nm SLM laser

When the incident pump power from LD2 remains at 2.3 W, the output power of MLM 589 nm and SLM 589 nm laser as a function of the LD1 incident pump power are shown in Fig.9. The maximum output power of MLM 589 nm and SLM 589 nm are 142 mW and 58 mW respectively when the LD1 power is 4.68 W. The possible reasons of that the output power of the SLM 589 nm laser is lower are as follows: First, there are extra insertion losses when the BP is placed in the cavity; Second, the pumping power of 1 319 nm is only 2.3W, which limits the sum-frequency efficiency.

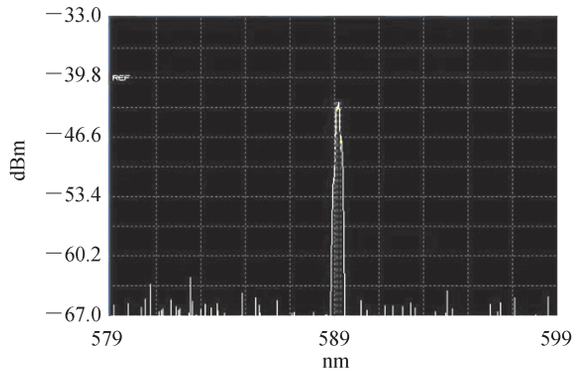

Fig.8 589 nm laser spectrum

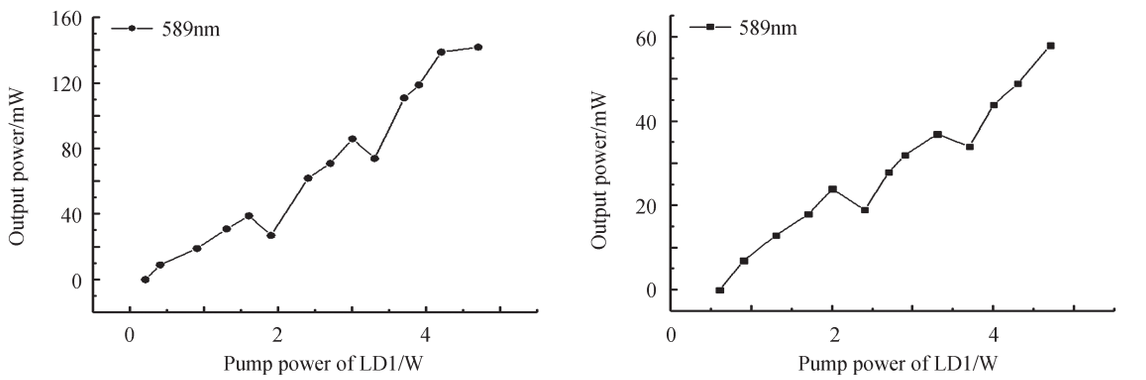

(a) 589 nm Multimode laser output power as a function of pump power of LD1 (LD2 keeps 2.3 W unchanged)

(b) 589 nm SLM laser output power as a function of pump power of LD1(LD2 keeps 2.3 W unchanged)

Fig.9 Output power of 589 nm as a function of the LD1 pump power

The stability experiment is conducted on an optical table in clean room at 25℃. The root-mean-square deviation is calculated to be 0.36% when the output power is at maximum, which is shown in Fig.10. The far-field spot of SLM 589 nm laser is measured, as shown in Fig.11, TEM_{00} single-transverse-mode operation is also confirmed.

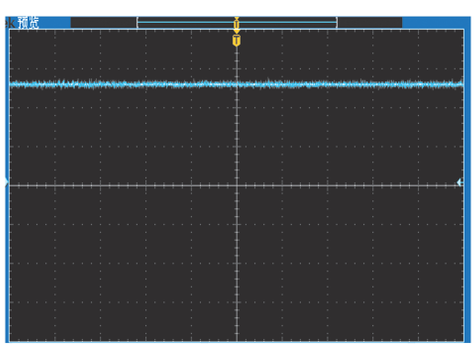

Fig.10 The amplitude fluctuation of SLM 589 nm output

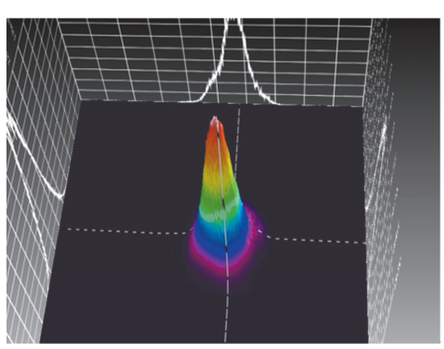

Fig.11 Diagram of SLM 589 nm laser far-field spot

3 Conclusion

We report an SLM 589 nm CW laser by using a birefringent filter consisted of single BP and KTP in the LD pumped composite-cavity. When the pumping powers of LDs are at maximum (1 064 nm resonator cavity with pump power at 4.68 W, 1 319 nm resonator cavity with pump power at 2.3 W), the SLM 589 nm yellow laser output power is 58 mW and the amplitude fluctuation is 0.36%. The line width of SLM 589 nm is 30 MHz. The experimental results show that longitudinal-mode-selective by a birefringent filter is an effective method for dual-wavelength oscillating laser. In fact, from Fig. 2 and Fig. 3 we can see that the larger the

adjacent longitudinal mode interval is, the larger the additional loss the first sub-longitudinal mode suffers. By designing the resonator as short as possible, it will be easier to realize SLM SFG laser. Composite-cavity scheme is very helpful to realize mode matching and also it is useful to get the perfect energy ratio between the two fundamental waves. With the advantage of avoiding competition between two fundamental waves and longitudinal coupling, our scheme is promising to achieve stable high power SLM laser.

Reference

[1] JEYS T H, BRAILOVE A, MOORADIAN A. Sum frequency generation of sodium resonance radiation[J]. Applied Optics,1989,28(13): 2588-2591.

[2] DANAILOV M B. 589 nm light generation by intracavity mixing in a Nd:YAG laser[J]. Journal of Applied Physics,1994, 75(12): 8240-8242.

[3] BI Yong, SUN Zhipei, ZHANG Ying, et al. All-solid-state sum-frequency 589 nm Nd:YAG laser[J]. Chinese Journal of Lasers,2003,5: 440

[4] BAER T. Large-amplitude fluctuation due to longitudinal-mode coupling in diode-pumped intracavity-doubled Nd: YAG laser[J]. Journal of the Optical Society of America B,1986, 3(9): 1175-1179.

[5] SURIN A A, BORISENKO T E, LARIN S V. Generation of 14 W at 589 nm by frequency doubling of high-power CW linearly polarized Raman fiber laser radiation in MgO:sPPLT crystal[J].Optics Letters, 2016,41(11): 2644-2647.

[6] LIU Yang, LIU Zhaojun. Quasi-continuous-wave 589-nm radiation based on intracavity frequency-doubled Nd: GGG/ BaWO4 Raman laser[J]. Optics and Laser Technology, 2016,81: 184-188.

[7] LI Mengmeng, YANG Fei, GAO Lanlan. All solid-state cavity and frequency single longitudinal mode 593.5nm yellow laser[J]. Chinese Journal of Lasers,2020,47(3): 0301003.

[8] BEGE R. Watt-level second-harmonic generation at 589 nm with a PPMgO:LN ridge waveguide crystal pumped by a DBR tapered diode laser[J]. Optics Letters,2016,41(7): 1530-1533.

[9] LU Huadong, PENG Kunchi. Realization of the single-frequency and high power as well as frequency tuning of the laser by manipulating the nonlinear loss [J]. Journal of Optics B-Quantum and Semiclassical Optics, 2015, 21(2): 171-176.

[10] WALLMEROTH K, PEUSER P. High power, cw single-frequency TEM_{00}, diode-laser pmped Nd: YAG laser[J]. Electronics Letters, 1988, 24(17): 1086-1088.

[11] ZAYHOWSKI J J, MOORADIAN A. Frequency-modulated Nd:YAG Microchip Lasers[J]. Optics Letters, 1989,14 (12):618-620.

[12] SUN Xuejun, WEI Jiao, WANG Wenzhe, et al. Realization of a continuous frequency-tuning Ti:sapphire laser with an intracavity locked etalon [J]. Chinese Optics Letters, 2015,13(7): 071401.

[13] TAN Wei, FU Xiaofang, LI Zhixin, et al. The wavelength tunable 589 nm laser output based on singly resonant sum-frequency generation and the measurement of saturate fluorescence spectrum of sodium atom [J]. Acta Physico Chimica Sinica,2013,62(9): 219-224.

[14] XIE Shiyong, ZHANG Xiaofu, YANG Chengliang, et al. Continuous-wave single-frequency 589 nm yellow laser generated from sum frequency of single-block non-planar ring cavity laser in periodically poled KTiOPO4 crystal [J]. Acta Physico Chimica Sinica,2016,65(9): 84-90.

[15] GAO Lanlan, TAN Huiming. LD-pumped all-solid-state single-frequency laser technology [J]. Optical Electromechanical Information,2002,(11):8-11.

[16] ABRAMOVICI A. Minimal Nd:YAP laser configuration with single frequency output[J]. Optics Communications,1987, 61(6): 401-404.

[17] LIU Xiaojuan , FU Lulian , ZHUO Ranran . Pulse LDA-pumped single-frequency Nd: YVO_4-KTP green laser using Brewster plate[J]. Journal of Optoelectronics Laser, 2006, 17:370-372.

[18] YUAN Yizhe, LI Bin. Laser diode-pumped Nd:YAG crystals frequency summing 589 nm yellow laser[J]. Optik,2016, 127(2):710-712.

[19] TUCKER A W, BIRNBAUM M, FINCHER C L, et al. Stimulated-emission cross-section at 1064 and 1342 nm in Nd: YVO4[J]. Journal of Applied Physics,1977,48(12): 4907-4911.

[20] XIE Shiyong, ZHANG Xiaofu. Continuous-wave single-frequency 589 nm yellow laser generated from sum-frequency of single-block non-planar ring cavity laser in periodically poled KTiOPO4 crystal[J]. Acta Physico Chimica Sinica,2016,65 (9): 094203.

[21] JUNGHANS J, KELLER M, WEBER H. Laser resonators with polarizing elements-Eigenstates and eigenvalues of polarization[J]. Applied Optics,1974,13(12): 2793-2798.